

An improved observable for the forward–backward asymmetry in $B \rightarrow K^* \ell^+ \ell^-$ and

$$B_s \rightarrow \phi \ell^+ \ell^-$$

Enrico Lunghi¹ and Amarjit Soni²

¹ *Physics Department, Indiana University, Bloomington, IN 47405, USA*
E-mail: elunghi@indiana.edu

² *Physics Department, Brookhaven National Laboratory,
 Upton, New York, 11973, USA*
E-mail: soni@bnl.gov

Abstract

We study the decay $B \rightarrow K^* \ell^+ \ell^-$ in the QCD factorization approach and propose a new integrated observable whose dependence on the form factors is almost negligible, consequently the non-perturbative error is significantly reduced and indeed its overall theoretical error is dominated by perturbative scale uncertainties. The new observable we propose is the ratio between the integrated forward–backward asymmetry (FBA) in the $[4, 6] \text{ GeV}^2$ and $[1, 4] \text{ GeV}^2$ dilepton invariant mass bins. This new observable is particularly interesting because, when compared to the location of the zero of the FBA spectrum, it is experimentally easier to measure and its theoretical uncertainties are almost as small; moreover it displays a very strong dependence on the phase of the Wilson coefficient C_{10} that is otherwise only accessible through complicated CP violating asymmetries. We illustrate the new physics sensitivity of this observable within the context of few extensions of the Standard Model (SM), namely the SM with four generations (SM4), an MSSM with non-vanishing source of flavor changing neutral currents in the down squark sector and a Z' model with tree level flavor changing couplings.

1 Introduction

The importance of the flavor-changing semileptonic decays, $b \rightarrow s(d)l^+l^-$ for searching effects of new physics has been recognized for a very long time [1–4]. The process is especially important because its amplitude is very sensitive to the presence of heavy virtual quarks, scaling as $(\text{mass}_{\text{quark}})^2$. The inclusive $\text{BR}(B \rightarrow X_s l^+ l^-) = (1.60 \pm 0.51) \times 10^{-6}$ is measured [5–7] and is consistent with the NNLO prediction of the Standard Model (SM), $(1.62 \pm 0.14) \times 10^{-6}$ with an accuracy of around 9% [8,9]; given the large experimental uncertainty, this measurement allows for new physics contributions at the $\sim 30\%$ level. The reaction is also of great interest as it offers numerous related observables through which to test the SM precisely and to discover new phenomena. The dilepton invariant mass (q^2) spectrum, forward-backward asymmetry (FBA) as function of q^2 , the location of the zero in the FBA and the possibility of searching for CP violation via, for example, partial rate asymmetry (PRA) are some of the attractive features of this reaction. As usual while theory predictions tend to be more reliable for inclusive modes, experimentally the related exclusive modes such as $B \rightarrow K(K^*)l^+l^-$, $B_s \rightarrow \phi l^+l^-$ are more readily accessible. A particular challenge for theory regarding these exclusive modes [10] is their dependence on form factors, which are manifestly properties of bound states and therefore of non-perturbative character. B factories of course have been able to study both inclusive and exclusive modes but at the LHCb inclusive studies seem rather difficult. On the other hand many of the exclusive modes are quite distinctive and in particular $B \rightarrow K^*l^+l^-$, $B_s \rightarrow \phi l^+l^-$ should be a focus of intense study at the LHCb and at the super-B factories.

In this paper, we will focus on the forward backward asymmetry in the q^2 distribution of $B \rightarrow K^*l^+l^-$, $B_s \rightarrow \phi l^+l^-$. The topic has gained renewed interest recently as measurements at BaBar [11], Belle [12] and CDF [13] all seem to show weak indications of deviations from expectations of the SM. Lack of statistics in these first observations may be the underlying reason but the prediction of the SM also has considerable uncertainties and that is a cause of some concern to which we will try to address in this work. As already mentioned the dominant source of the uncertainties is the form-factor dependence; these are not amenable to perturbation theory and improvement using non-perturbative methods tends to be rather slow.

Here we propose the ratio of the integrated forward–backward asymmetry in the $[4, 6]$ GeV^2 and $[1, 4]$ GeV^2 q^2 regions (just above and below the location of the zero of the spectrum). In this ratio, the form factors uncertainties cancel to a great extent and the total error is controlled by scale uncertainties whose perturbative origin allows for future improvements.

2 $B \rightarrow K^* \ell \ell$ in QCD factorization

The effective Hamiltonian responsible for the short distance $b \rightarrow s \ell^+ \ell^-$ transition is

$$\mathcal{H}_{\text{eff}}^{b \rightarrow s \ell \ell} = -\frac{4G_F}{\sqrt{2}} V_{tb} V_{ts}^* \left[\sum_{i=1}^6 C_i O_i + \sum_{i=3}^6 C_{iQ} O_{iQ} + C_b O_b + \sum_{i=7,8,S,P} (C_i O_i + C'_i O'_i) \right]$$

$$+ \frac{\alpha_e}{4\pi} \sum_{i=9,10} (C_i O_i + C'_i O'_i) \Big] \quad (1)$$

where the definition of the operators and the corresponding SM matching conditions can be found in Ref. [8,14]*. Primed operators are obtained from the unprimed ones by the substitution $L \leftrightarrow R$. The electroweak penguin and O_b operators contributions to $B \rightarrow K^* \ell \ell$ can be neglected because their impact is much smaller than the overall theory uncertainty.

It is possible to show that, for small values of the dilepton invariant mass ($q^2 \lesssim 6 \text{ GeV}^2$), the $B \rightarrow K^* \ell \ell^\dagger$ matrix element of all the operators appearing in Eq. (1) obey the following factorization formula [15]:

$$\langle K_a^* \ell \ell | O_i | B \rangle = C_a^i \xi_a(q^2) + \sum_{\pm} \int d\omega du T_{a,\pm}^i(q^2, u, \omega) \Phi_{B,\pm}(\omega) \Phi_{K^*}(u) + O(\Lambda_{QCD}/m_b) \quad (2)$$

where $a = \perp, \parallel$ refers to the transverse (longitudinal) polarization of the K^* , ξ_a are soft form factors and $\Phi_{B,\pm}$ and Φ_{K^*} are the light cone wave functions of the B and K^* mesons. The quantities C_a^i and $T_{a,\pm}^i$ can be calculated in perturbation theory.

$B \rightarrow K^* \ell \ell$ matrix elements can be decomposed using a basis of eight transversity amplitudes (see, for instance, the discussion in Sec. 3.2 of Ref. [14]): $A_{\perp L,R}$, $A_{\parallel L,R}$, $A_{0L,R}$, A_t and A_S . In this notation, A_{\perp} and A_{\parallel} correspond to the two possible transverse polarization states of the K^* and are described by the form factor ξ_{\perp} ; A_0 , A_t and A_S involve a longitudinally polarized K^* and are described in terms of ξ_{\parallel} .

Up to electromagnetic corrections, the various $B \rightarrow K^* \ell \ell$ matrix elements of the semileptonic and magnetic moment operators $O_{7,9,10}^{(\prime)\dagger}$ can be exactly expressed in terms of the seven form factors $V(q^2)$, $A_{1,2,3}(q^2)$ and $T_{1,2,3}(q^2)$. Up to power corrections, these form factors can be written as the sum of soft and hard factorizable contributions using Eq. (2). It is important to realize that the separation between soft and hard contributions is subject to a certain degree of arbitrariness; therefore it is necessary to choose a factorization scheme and adopt precise definitions of the soft form factors in terms of the full QCD ones. Following the analysis of Ref. [16] we adopt the following definitions:

$$\xi_{\perp}(q^2) = \frac{m_B}{m_B + m_{K^*}} V(q^2) \quad \text{and} \quad \xi_{\parallel}(q^2) = \frac{m_B + m_{K^*}}{2E_{K^*}} A_1(q^2) - \frac{m_B - m_{K^*}}{m_B} A_2(q^2). \quad (3)$$

The form factors V , A_1 and A_2 are taken from the Light-Cone Sum Rule analysis of Refs. [14,17]. In the numerical analysis we vary independently the $q^2 = 0$ values of the two soft form factors ξ_{\perp} and ξ_{\parallel} over the one-sigma errors given in Table 1. The matrix elements of all the other operators do not admit a simple interpretation in terms of form factors but can be expressed using Eq. (2) in which ξ_{\perp} and ξ_{\parallel} are the same soft form factors introduced in Eq. (3).

*Note that here we adopt a more conventional definition of the semileptonic operators $O_{9,10}$ and, unlike Ref. [8], we factor out $\alpha_e/4\pi$ in their definition so that their Wilson coefficients start at order $O(\alpha_s^0, \alpha_e^0)$.

‡For definiteness, we will continue to explicitly mention $B \rightarrow K^* \ell^+ \ell^-$ only, however, it should be obvious that our equations and the ensuing discussions are applicable equally well to $B_s \rightarrow \phi \ell^+ \ell^-$.

†This applies also to the matrix elements of the scalar and pseudoscalar operators $O_{S,P}^{(\prime)}$.

Let us now sketch how all the different parts of this calculation come together. Up to $O(\alpha_s)$ corrections, the three most relevant transversity amplitudes are schematically given by

$$A_{\perp L,R} \propto [(C_9^{\text{eff}} + C'_9) \mp (C_{10} + C'_{10})] V(q^2) + \frac{2m_b m_B}{q^2} (C_7 + C'_7) T_1(q^2) \quad (4)$$

$$A_{\parallel L,R} \propto [(C_9^{\text{eff}} - C'_9) \mp (C_{10} - C'_{10})] A_1(q^2) + \frac{2m_b m_B}{q^2} (C_7 - C'_7) T_2(q^2) \quad (5)$$

$$A_{0L,R} \propto [(C_9^{\text{eff}} - C'_9) \mp (C_{10} - C'_{10})] \{A_1(q^2), A_2(q^2)\} + (C_7 - C'_7) \{T_1(q^2), T_2(q^2)\} \quad (6)$$

where $\{\cdot, \cdot\}$ indicates a linear combination, $C_9^{\text{eff}} = C_9 + Y(q^2)$ and $Y(q^2)$ is the sum of the leading order matrix elements of the current–current and QCD penguin operators O_{1-6} and can be found for instance in Ref. [15]. All Wilson coefficients are evaluated at a scale $\mu_b \sim m_b$. Complete expressions for the eight transversity amplitudes can be found in Refs. [14, 18, 19].

Part of the $O(\alpha_s)$ corrections are buried inside the form factors; therefore the first step consists in replacing each form factor with the corresponding QCD factorization expansion (e.g. $V = \xi_{\perp} (m_B + m_{K^*})/m_B$). The complete expansion of the form factors in terms of $\xi_{\perp, \parallel}$ can be found in Refs. [15, 16, 20]. In a second step all the remaining non-factorizable corrections originating from the remaining operators (other than $O_{7,9,10}$) have to be included. Since the latter can always be described in terms of $B \rightarrow K^* \gamma^*$ matrix elements it is customary to lump them together in some effective photonic form factors:

$$(C_7 - C'_7) T_i(q^2) \rightarrow \tau_i^-(q^2) \quad (7)$$

$$(C_7 + C'_7) T_i(q^2) \rightarrow \tau_i^+(q^2), \quad (8)$$

where the index \pm refers to the combinations $C_7 \pm C'_7$. The quantities τ_i^{\pm} are obtained from the τ_i introduced in Ref. [15] with the appropriate $C_7 \rightarrow C_7 \pm C'_7$ substitution. Following Ref. [15], the contribution from the $Y(q^2)$ term in C_9^{eff} is also included in the τ_i ; therefore we also have to replace $C_9^{\text{eff}} \rightarrow C_9$.

Note that the factorization scheme that we adopt implies the absence of $O(\alpha_s)$ corrections to the form factors $V(q^2)$, $A_1(q^2)$ and $A_2(q^2)$ (that are therefore simply expressed in terms of the soft form factors $\xi_{\perp, \parallel}$ without any $O(\alpha_s)$ contribution). The form factor $A_0(q^2)$, on the other hand, receives non-trivial $O(\alpha_s)$ corrections. Effects on the photonic form factors $T_i(q^2)$ are included in the definition of the τ_i^{\pm} .

Once the transversity amplitudes have been calculated at order α_s , it is trivial to express the fully differential $B \rightarrow K^*(\rightarrow K\pi)\ell\ell$ decay width. In the limit $m_{\ell} \rightarrow 0$, one finds:

$$\frac{d\Gamma}{dq^2 d\cos\theta_{\ell}} = \frac{3}{4} \left(I_1^c + 2I_2^s + (2I_2^s - I_1^c) \cos^2\theta_{\ell} + I_6^s \cos\theta_{\ell} \right) \quad (9)$$

where

$$I_2^s = \frac{1}{4} (|A_{\perp}^L|^2 + |A_{\parallel}^L|^2 + |A_{\perp}^R|^2 + |A_{\parallel}^R|^2) \quad (10)$$

$$I_1^c = |A_0^L|^2 + |A_0^R|^2 \quad (11)$$

$$I_6^s = 2 \text{Re} (A_{\parallel}^L A_{\perp}^{L*} - A_{\parallel}^R A_{\perp}^{R*}) \quad (12)$$

$m_b^{1S} = (4.68 \pm 0.03) \text{ GeV}$ [21]	$m_c(m_c) = (1.27_{-0.11}^{+0.07}) \text{ GeV}$ [22]
$\xi_{\perp}(0) = 0.266 \pm 0.032$ [14, 17]	$\xi_{\parallel}(0) = 0.118 \pm 0.008$ [14, 17]
$f_B = (192.8 \pm 9.9) \text{ MeV}$ [23]	$f_{k^*}^{\perp} = (163 \pm 8) \text{ MeV}$ [24]
$f_{k^*}^{\parallel} = (220 \pm 5) \text{ MeV}$ [24]	$a_1^{\perp, \parallel} = 0.03 \pm 0.03$ [24]
$a_2^{\perp, \parallel} = 0.08 \pm 0.06$ [24]	$\lambda_B = (0.51 \pm 0.12) \text{ GeV}$ [17]

Table 1: Inputs used in the numerical analysis of the forward–backward asymmetry. All other inputs are taken from the PDG [22].

where θ_{ℓ} is the angle between the ℓ^+ and the B in the dilepton centre of mass system. Complete expressions for the differential decay width and the twelve I_i^a functions can be found in Ref. [14]. The forward–backward asymmetry is obtained integrating Eq. (9) over $\cos \theta_{\ell}$:

$$\mathcal{A}_{\text{FB}}(q^2) \equiv \frac{\int \frac{d\Gamma}{dq^2 d\cos\theta_{\ell}} \text{sgn}(\cos\theta_{\ell}) d\cos\theta_{\ell}}{\int \frac{d\Gamma}{dq^2 d\cos\theta_{\ell}} d\cos\theta_{\ell}} = \frac{3}{4} \frac{I_6^s}{I_1^c + 4I_2^s}. \quad (13)$$

Using Eqs. (4,5,12,13) and the leading order expressions for the form factors, one finds that the numerator of the forward–backward asymmetry is proportional to

$$-\xi_{\perp}^2 \text{Re} \left\{ C_{10}^* \left(C_9^{\text{eff}}(q^2) + 2 \frac{m_b m_B}{q^2} C_7 \right) \right\} + O(\alpha_s, \Lambda/m_b). \quad (14)$$

At order $O(\alpha_s^0)$ this quantity does not depend on the form factor ξ_{\parallel} . For this reason hadronic uncertainties affect the location of zero of the \mathcal{A}_{FB} spectrum

$$q_0^2 \simeq -2m_b m_B \frac{C_9^{\text{eff}}(q_0^2)}{C_7} + O(\alpha_s, \Lambda/m_b) \quad (15)$$

only at the NLO level. Note that this statement does not extend to integrals of the forward–backward asymmetry over an arbitrary q^2 interval. In fact the denominator of Eq. (13), i.e. the differential rate, depends at leading order on both soft form factors through the transversity amplitude $A_{0L,R}$: at this order the form factors V , A_0 , T_1 and T_2 are proportional to ξ_{\perp} and the form factor A_2 is proportional to $\xi_{\perp} - \xi_{\parallel}$. The uncertainty on our knowledge of these two form factors is the dominant source of uncertainty on the forward–backward asymmetry spectrum and various integrals. In Table 1 we summarize the inputs that we need for a complete numerical analysis of the forward–backward asymmetry; note that the $\xi_{\perp, \parallel}(0)$ are taken from Ref. [14, 17] from where the q^2 dependence of the form factors is also taken.

In Fig. 1 we plot the differential forward–backward asymmetry in the $1 \text{ GeV}^2 < q^2 < 6 \text{ GeV}^2$ range. The blue shaded area in the first panel indicates the total uncertainty that we obtain by varying all the input parameters given in table 1 and the factorization scale μ_b . The latter dependence is an artifact and can be reduced by including higher order terms of the perturbative α_s expansion. In this paper we allow μ_b to vary in the usual $[m_b^{\text{pole}}/2, 2m_b^{\text{pole}}]$ range (but also

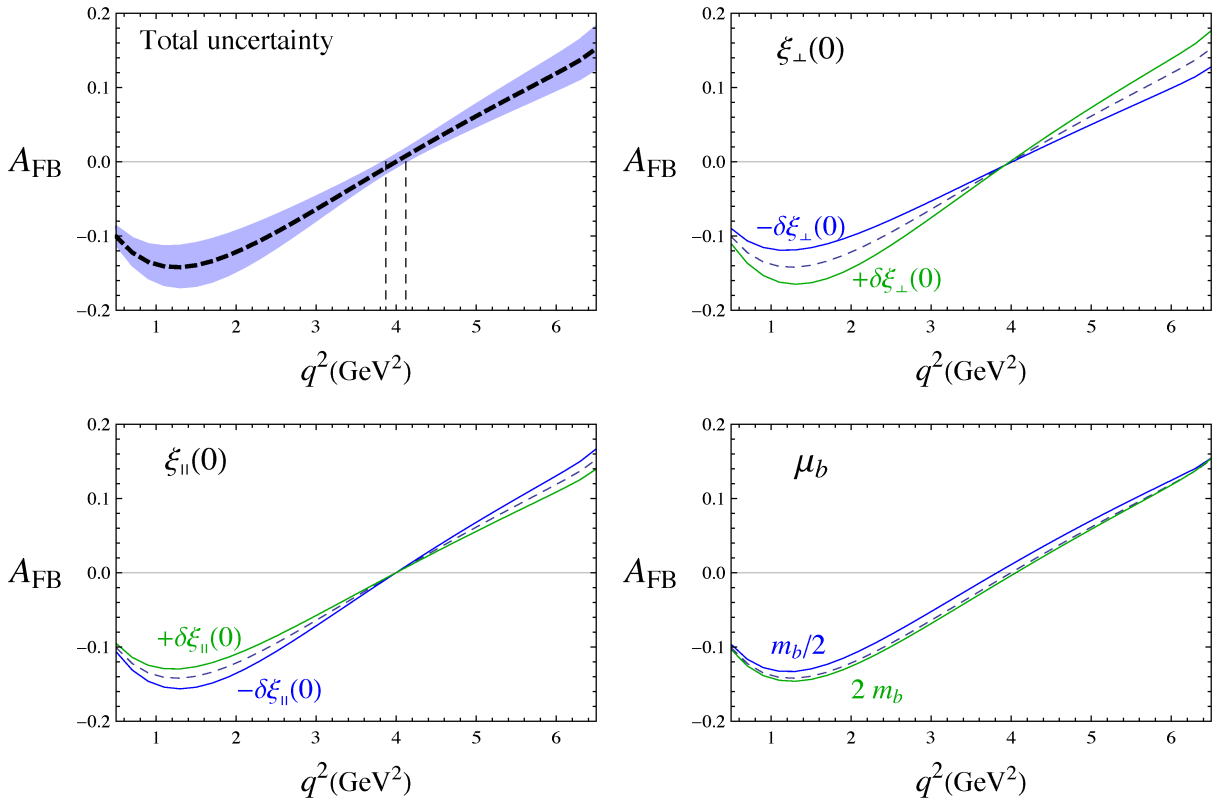


Figure 1: Error analysis of the forward–backward asymmetry spectrum. In the first panel we present the total error on the FBA spectrum obtained by adding all sources of uncertainty in quadrature. In the remaining panels we show the errors induced separately by the two soft form factors and by the variation of the low–scale μ_b .

present the results we obtain for the more conservative $[4, 5.6]$ GeV range adopted in Ref. [14]). The location of the zero of the forward–backward asymmetry spectrum is $q_0^2 = (4.0 \pm 0.13)$ GeV². In the other three panels we show separately the impact of the three most important sources of uncertainties. Note that the variation of the scale μ_b at which the Wilson coefficients are evaluated induces a constant shift on the whole spectrum and that the uncertainties on the $q^2 = 0$ values of the soft form factors switch sign above and below q_0^2 .

The latter observation leads us to propose a new integrated observable for which we expect a very tiny form factor uncertainty, namely the ratio between the the forward–backward asymmetry integrated in the $[4, 6]$ GeV² and $[1, 4]$ GeV² bins:

$$\mathcal{R}[q_0^2] = \frac{\int_{q_0^2}^6 \mathcal{A}_{\text{FB}}(q^2) dq^2}{\int_1^{q_0^2} \mathcal{A}_{\text{FB}}(q^2) dq^2}. \quad (16)$$

The SM predictions for the integrated forwards–backward asymmetry in the two low- q^2 bins

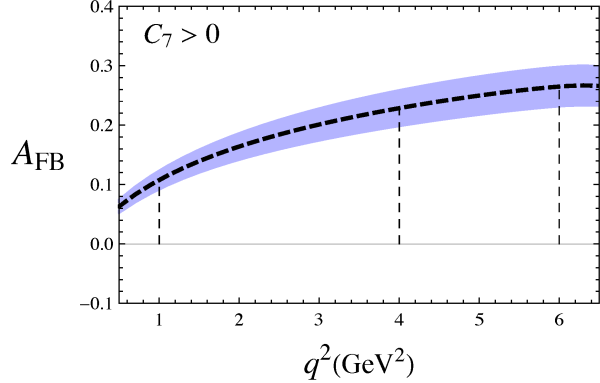


Figure 2: Error analysis of the forward–backward asymmetry spectrum for $C_7 > 0$.

and for the ratio $\mathcal{R}[q_0^2]$ are:

$$\int_1^4 \mathcal{A}_{\text{FB}}(q^2) dq^2 = -0.089 (1 \pm 0.085_{\mu_b} \pm 0.17_{\xi_{\perp}(0)} \pm 0.10_{\xi_{\parallel}(0)} \pm 0.031_{\text{rest}}) \quad (17)$$

$$= -0.089 \pm 0.020 [22\%], \quad (18)$$

$$\int_4^6 \mathcal{A}_{\text{FB}}(q^2) dq^2 = 0.062 (1 \pm 0.089_{\mu_b} \pm 0.18_{\xi_{\perp}(0)} \pm 0.10_{\xi_{\parallel}(0)} \pm 0.067_{\text{rest}}) \quad (19)$$

$$= 0.062 \pm 0.015 [24\%], \quad (20)$$

$$\mathcal{R}[4] = -0.701 (1 \pm 0.19_{\mu_b} \pm 0.012_{\xi_{\perp}(0)} \pm 0.0057_{\xi_{\parallel}(0)} \pm 0.083_{\text{rest}}) \quad (21)$$

$$= -0.701 \pm 0.15 [21\%]. \quad (22)$$

where the suffix “rest” stands for variations of m_b , m_c , f_B , $f_{K^*}^{\perp,\parallel}$, $a_{1,2}^{\perp,\parallel}$ and λ_B . Note, in particular, that form factors uncertainties on $\mathcal{R}[q_0^2]$ are vanishingly small while the impact of all other sources of uncertainty is enhanced. The basic reason behind this behavior is that the effect of any parameter with the exception of the two soft form factors is a parallel shift of the whole forward–backward asymmetry spectrum, thus enhancing their impact on the ratio $\mathcal{R}[q_0^2]$. Adopting the narrower variation $\mu_b \in [4, 5.6]$ GeV suggested in Ref. [14], the scale uncertainties in Eqs. (17, 19, 21) shift from (8.5%, 8.9%, 19%) to (2%, 2%, 4%); consequently the total uncertainties in Eqs. (18, 20, 22) shift from (0.020, 0.015, 0.15) to (0.018, 0.014, 0.07). The impact of this more restricted scale variation is fairly small on the integrated FBA in the two bins because the total uncertainty is dominated by the form factors. On the other hand, $\delta\mathcal{R}[4]$ is controlled by the scale variation and, as we explained above, the scale uncertainties in Eqs. (17) and (19) are anticorrelated. There are three main arguments in favor of adopting the observable that we propose.

- $\mathcal{R}[q_0^2]$ is sensitive to the same combinations of Wilson coefficients that determine the position of the zero of the spectrum but it is much simpler to determine experimentally. Moreover, it can be measured even in presence of new physics that removes entirely the zero from the spectrum.

- The dominant source of uncertainty on $\mathcal{R}[q_0^2]$ is the scale at which the Wilson coefficients are evaluated. Within the QCD factorization approach this dependence can be reduced by NNLO perturbative calculations and can, therefore, be brought under control.
- The branching ratio and the location of zero of the FBA spectrum are completely insensitive to the phase of the Wilson coefficient C_{10} . In fact, the FBA is proportional to C_{10} and the location of the zero depends only on $|C_{10}|$. The integrated forward-backward asymmetry dependence on this phase is, on the other end, non trivial. This can be understood by looking once more at the LO expression for the numerator of the forward-backward asymmetry for arbitrary complex Wilson coefficients:

$$\mathcal{A}_{\text{FB}}(q^2) \propto \text{Re} \left\{ C_{10}^* \left(C_9 + Y(q^2) + 2 \frac{m_b m_B}{q^2} C_7 \right) \right\} \quad (23)$$

$$= \text{Re} \left\{ |C_{10}| e^{-i\phi_{10}} \left(|C_9| e^{i\phi_9} + Y(q^2) + 2 \frac{m_b m_B}{q^2} |C_7| e^{i\phi_7} \right) \right\} \quad (24)$$

$$= |C_{10}| \left[\cos(\phi_{10} - \phi_9) |C_9| + \cos \phi_{10} \text{Re} Y(q^2) + \cos(\phi_{10} - \phi_7) 2 \frac{m_b m_B}{q^2} |C_7| + \sin \phi_{10} \text{Im} Y(q^2) \right], \quad (25)$$

where we remind the reader that in the SM we have $\phi_{10} = \phi_9 = 0$ and $\phi_7 = \pi$. Eq. (25) displays explicitly the dependence of the integrated FBA on ϕ_{10} . Unfortunately an effect here can always be reabsorbed into a change of the absolute value and sign of this coefficient (note that the FBA is actually proportional to $|C_{10}|$). We note also that the FBA is a parity odd observable that can be decomposed into CP even and odd components, the latter being the term proportional to $\sin \phi_{10}$. From the inspection of Eq. (25) we immediately see that the ratio $\mathcal{R}[q_0^2]$ is completely insensitive to $|C_{10}|$ (there is a mild residual dependence of $\mathcal{R}[q_0^2]$ on $|C_{10}|$ through the denominator of the FB asymmetry); in contrast, the dependence on the phase of C_{10} is quite strong and it arises through the interference with the strong phase in the matrix elements of the QCD penguin operators (the imaginary part of $Y(q^2)$ for $q^2 < 4m_c^2$ originates from the QCD penguin matrix elements involving a light quark loop and is independent of q^2 in the limit of vanishing light quark masses [25]).

Let us consider the simpler scenario of vanishing new physics weak phases in C_7 and C_9 . In this case we have:

$$\mathcal{A}_{\text{FB}}(q^2) \propto |C_{10}| \cos \phi_{10} \left[|C_9| + \text{Re} Y(q^2) + 2 \frac{m_b m_B}{q^2} |C_7| + \tan \phi_{10} \text{Im} Y(q^2) \right]. \quad (26)$$

Integrating over the $[1, 4]$ GeV² and $[4, 6]$ GeV² ranges and assuming the SM values for the coefficients $C_{7,9}$ we obtain (formulas valid at NLO will be presented in the next section):

$$\mathcal{R}[4] \propto \frac{\int_4^6 \mathcal{A}_{\text{FB}}(q^2) dq^2}{\int_1^4 \mathcal{A}_{\text{FB}}(q^2) dq^2} \propto -\frac{1 + 0.13 \tan \phi_{10}}{1 - 0.03 \tan \phi_{10}}. \quad (27)$$

	HN	HD	LN	LD
q_0	2.672	60.55	-5.425	42.97
q_{77}	0	124.6	0	38.95
q_{88}	0	0.7053	0	0.2085
q_{99}	0	1.967	0	1.548
q_{1010}	0	1.954	0	1.540
q_7	23.98	-21.65+8.820 i	35.42	23.23+3.561 i
q_8	1.159+1.260 i	-1.120-0.1590 i	1.798+1.859 i	1.142+1.521 i
q_9	2.694	9.969+0.3029 i	1.993	9.110+0.3954 i
q_{10}	-0.6372-0.2986 i	-16.38	1.294-0.3303 i	-12.92
q_{78}	0	13.02-13.37 i	0	3.878-4.161 i
q_{79}	0	17.90	0	12.03
q_{710}	-5.718	0	-8.446	0
q_{89}	0	1.042+1.088 i	0	0.6379+0.6671 i
q_{810}	-0.2763-0.3005 i	0	-0.4288-0.4432 i	0
q_{910}	-0.6424	0	-0.4754	0

Table 2: Coefficients q_i and q_{ij} .

A very interesting feature of Eq. (27) is that, in this scenario, the difference between $\mathcal{R}[4]$ and its SM expectation is proportional to $\tan \phi_{10}$. This behavior is usually displayed only by CP violating quantities; for instance, the CP asymmetry in the forward–backward asymmetry studied in Ref. [26] is proportional to $\text{Im } C_{10} = |C_{10}| \sin \phi_{10}$ (see Eq. (6.10) in Ref. [26]). The ratio $\mathcal{R}[4]$ retains this dependence on ϕ_{10} but is independent of $|C_{10}|$. Therefore we conclude that $\mathcal{R}[4]$ not only complements the branching ratio and the location of the zero of the spectrum but also provide a unique and direct access to the phase of C_{10} .

Let us now discuss scenarios in which the spectrum of the forward–backward asymmetry does not contain a zero. In this case all sources of uncertainties simply shift the spectrum (see Fig. 2) and the ratio $\mathcal{R}[4]$ turns out to be extremely clean. For illustration, we choose $\delta C_7(\mu_b) \simeq 1.15$ (this value reproduces the central value of the experimental determination of $B \rightarrow X_s \gamma$) and obtain:

$$(\mathcal{R}[4])_{C_7 > 0} = 1.42 \pm 0.04, \quad (28)$$

showing significant reduction in the error.

Finally we summarize the present experimental determination of the $B \rightarrow K^* \ell^+ \ell^-$ forward–backward asymmetry and attempt a first comparison with the SM prediction. The main limitation we encounter is that the Belle [12] and CDF [13] collaborations[†] present results in the whole low dilepton invariant mass region ($0 < m_{\ell\ell} < 8.68 \text{ GeV}^2$) including regions (i.e. $m_{\ell\ell} < 1 \text{ GeV}^2$

[†]The BaBar collaboration published a study of the integrated FBA in the whole low q^2 region [11], without giving separate results for the q^2 bins we are interested in in this work.

and $m_{\ell\ell} > 6 \text{ GeV}^2$) in which the theory approach we are adopting is subject to larger uncertainties. The Belle and CDF results, their weighted average and the corresponding SM predictions, with the caveat we just mentioned, read (the suffixes refer to the q^2 bin expressed in GeV^2):

	$\mathcal{A}_{\text{FB}}^{[0,2]}$	$\mathcal{A}_{\text{FB}}^{[2,4.3]}$	$\mathcal{A}_{\text{FB}}^{[4.3,8.68]}$
Belle	$0.47_{-0.32}^{+0.26} \pm 0.03$	$0.11_{-0.36}^{+0.31} \pm 0.07$	$0.45_{-0.21}^{+0.15} \pm 0.15$
CDF	$0.13_{-0.75}^{+1.65} \pm 0.25$	$0.19_{-0.41}^{+0.40} \pm 0.14$	$-0.06_{-0.28}^{+0.30} \pm 0.05$
Average	0.45 ± 0.28	0.12 ± 0.27	0.24 ± 0.23
SM	-0.027 ± 0.004	-0.050 ± 0.012	0.133 ± 0.026

Given our ignorance of the correlations between the experimental uncertainties in the various bins, we are unable to extract meaningful constraints on the ratios we are interested in.

3 Model independent analysis

Let us start by presenting a numerical formula that allows to calculate the integrated observable $R[4 \text{ GeV}^2]$ for arbitrary values of the complex Wilson coefficients $C_{7,8,9,10}(\mu_b) = C_{7,8,9,10}^{\text{SM}}(\mu_b) + \delta C_{7,8,9,10}$. We write:

$$R[4] = \frac{f_{\text{HN}}}{f_{\text{HD}}} / \left(\frac{f_{\text{LN}}}{f_{\text{LD}}} \right) \quad (29)$$

$$f_q = q_0 + \sum_{i=7}^{10} \text{Re}[q_i \delta C_i] + \sum_{i \leq j=7}^{10} \text{Re}[q_{ij} \delta C_i \delta C_j^*] \quad (30)$$

where in the suffixes AB, A = L, H stands for the low ($[1, 4] \text{ GeV}^2$) or high ($[4, 6] \text{ GeV}^2$) bin and B = N, D stands for the numerator or denominator of the forward-backward asymmetry; therefore f_{HN} (f_{LN}) and f_{HD} (f_{LD}) correspond to the integral of the numerator and denominator of the forward-backward asymmetry in the $[4, 6] \text{ GeV}^2$ ($[1, 4] \text{ GeV}^2$) range. The complex coefficients q_i and q_{ij} are given in Table 2.

In the following we will adopt the numerical formulas for $\text{BR}(B \rightarrow X_s \gamma)$ and $\text{BR}(B \rightarrow X_s \ell^+ \ell^-)$ presented in Refs. [8, 19]; the experimental determinations of these two branching ratios can be found in Refs. [27–34] and their world averages are given, for instance, in Refs. [5–7].

As we discussed in the previous section, although $\mathcal{R}[q_0^2]$ is an intrinsically CP conserving observable, the interference between weak and strong phases in the numerator of the forward-backward asymmetry introduces a strong sensitivity to new physics CP violating phases[‡]. Especially interesting is the sensitivity to the elusive phase of C_{10} . We present the result of a model independent study of new physics contributions to C_7 , C_9 and C_{10} in Figs. 3-4. When allowing for complex contributions to δC_i , we force the phases to lie in the $[-\pi/2, \pi/2]$ range and write $\delta C_i = \pm |\delta C_i| e^{i\phi_i}$ where $\phi_i = \arg \delta C_i$ or $(\arg \delta C_i - \pi) \bmod 2\pi$. In the upper panels of Fig. 3 we

[‡]The impact of CP violating phases in the denominator of the FBA, i.e. the branching ratio, is much smaller and essentially confined to the interference between C_7 and C_9 .

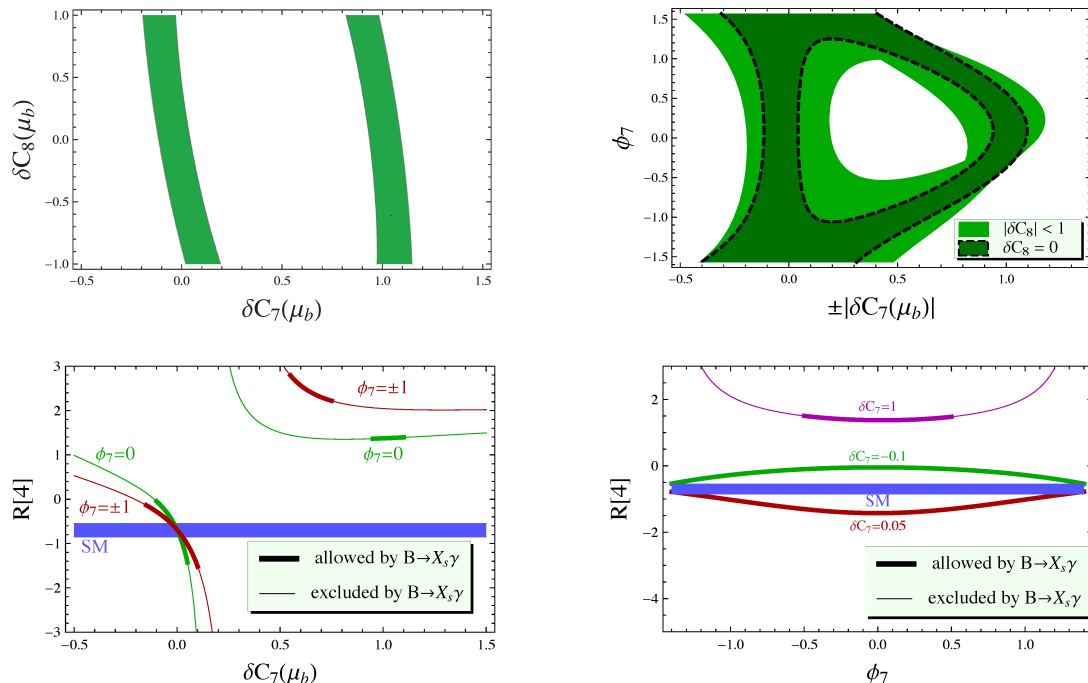


Figure 3: *Upper panels.* 95% C.L. regions allowed by $B \rightarrow X_s \gamma$ in the $[\delta C_7, \delta C_8]$ (for real δC_i) and complex δC_7 planes. *Lower panels.* Dependence of $\mathcal{R}[4]$ on the Wilson coefficients C_7 .

show bounds implied by $B \rightarrow X_s \gamma$ on the NP contributions $\delta C_7(\mu_b)$ and $\delta C_8(\mu_b)$. In the left panel we consider real coefficients and in the right one we entertain the complex δC_7 scenario. The two distinct regions that are allowed in the left panel correspond to the two possible signs for the $b \rightarrow s \gamma$ amplitude that is approximately proportional to $C_7(\mu_b) = C_7^{\text{SM}}(\mu_b) + \delta C_7(\mu_b)$, with $C_7^{\text{SM}}(\mu_b) < 0$. The precise experimental determination of $\text{BR}(B \rightarrow X_s \gamma)$ implies that δC_7 can lie either in a small region around 0 (same sign solution, $C_7 \sim C_7^{\text{SM}} < 0$) or in a narrow band around $\delta C_7 \sim 1$ (opposite sign solution, $C_7 \sim -C_7^{\text{SM}} > 0$). In the two lower panels of Fig. 3 we show the dependence of $\mathcal{R}[4]$ on the complex coefficient δC_7 ; the parts of the curves that are actually allowed by the $B \rightarrow X_s \gamma$ constraint are indicated by thicker lines. From the inspection of these plots we see that these effects do not depend much on possible NP phases in δC_7 and that for the same sign solution $C_7 < 0$, moderately large effects are possible. The opposite sign solution $C_7 > 0$ yields a change in the sign of $\mathcal{R}[4]$ but is currently disfavored by $B \rightarrow X_s \ell^+ \ell^-$ data.

In Fig. 4 we present a similar analysis for NP effects on C_9 and C_{10} . Note that, in the absence of extra phases, $\mathcal{R}[4]$ is almost completely insensitive to $|\delta C_{10}|$. Note the contrast between complex effects in C_9 and C_{10} . In the former case the impact of a non-vanishing ϕ_9 can be sizable but not essential in order to obtain large effects on $\mathcal{R}[4]$; in the latter case, the condition $\phi_{10} \neq 0$ is necessary in order to have an effect at all.

An interesting feature of these plots is the appearance of very large effects on $\mathcal{R}[4]$ for certain values of the coefficients $C_{7,9}$. Positive new physics contributions to $C_{7,9}$ tend to shift the zero

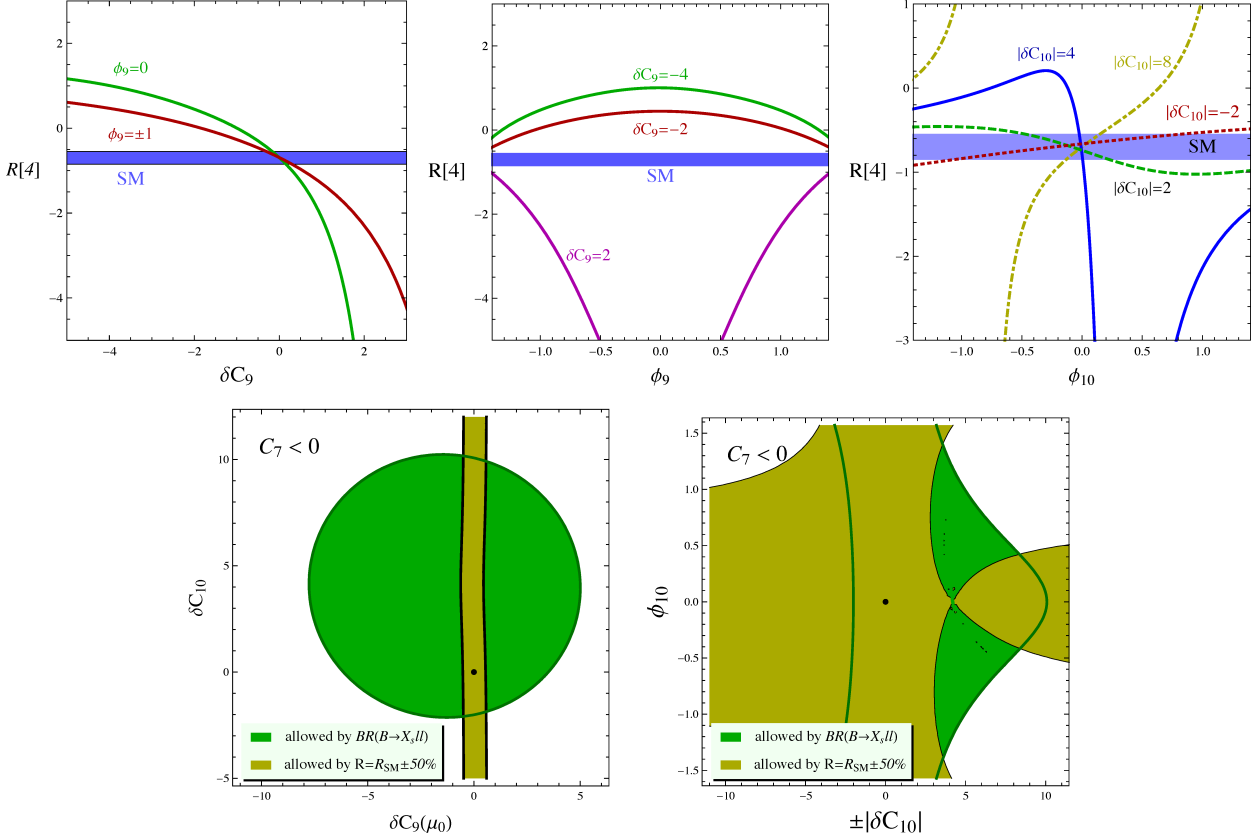


Figure 4: *Upper panels.* Dependence of $\mathcal{R}[4]$ on the Wilson coefficients C_9 and C_{10} . *Lower panels.* Bounds on the Wilson coefficients $C_{9,10}(\mu_b)$ from $B \rightarrow X_s ll$ (dark green regions) and from a possible measurement of the ratio $R[4]$ (light green regions). We fix C_7 to its SM value and assume $R[4]_{\text{exp}} = R[4]_{\text{SM}} \pm 50\%$.

of the FB asymmetry towards smaller q^2 values. The integral of $\mathcal{AFB}(q^2)$ in the $[1, 4]$ GeV² range receives, therefore, positive and negative contributions and, for some value of the Wilson coefficients, it can vanish. At this point the ratio $\mathcal{R}[4]$ can become very large and one may need to adopt a different strategy (e.g. consider $\mathcal{R}[q^2]$ for some other q^2 value).

It is particularly interesting to extract the bounds on δC_9 and δC_{10} that follow from a hypothetical measurement of $\mathcal{R}[4]$. In the lower panels of Fig. 4 we assume an experimental determination of the ratio $\mathcal{R}[4]$ with an uncertainty of 50% and central values agreeing with the SM and study its impact on the real $[\delta C_9, \delta C_{10}]$ and in the complex δC_{10} planes. In these plots the shaded disks represent the area allowed by $\mathcal{B}(B \rightarrow X_s \ell \ell)$ and the light shaded areas are the region of the $[C_9, C_{10}]$ plane that is selected by the measurement of $\mathcal{R}[4]$.

From the inspection of the lower-left panel of Fig. 4 we conclude that even a relatively poor determination of $\mathcal{R}[4]$ can help hugely in determining the value of C_9 . The lower-right panel of Fig. 4 illustrates the impact of a complex phase in δC_{10} : as long as $\phi_{10} \neq 0$ a determination of $\mathcal{R}[4]$ strongly constraints $|\delta C_{10}|$.

4 Few concrete examples

In this section we briefly entertain three distinct new physics scenarios and investigate the role of a measurement of $\mathcal{R}[4]$ on their phenomenology. In Sec. 4.1 we consider the addition of a fourth generation to the SM. In Sec. 4.2 we discuss one supersymmetric extension of the SM: an R -parity conserving MSSM with extra sources of flavor changing interactions in the down squark sector. In Sec. 4.3 we consider a family-dependent $U(1)'$ model. Note that in the 4th generation and Z' models the effects are driven by new CP violating phases in C_{10} ; in the SUSY scenario, the effect is controlled by more traditional contributions to the (chromo-)magnetic moment coefficients $C_{7,8}$.

4.1 4th generation

The inclusion of a fourth generation is perhaps the simplest extension of the Standard Model. The phenomenology of this model, usually referred as SM4, has recently been the subject of intensive scrutiny (see, for instance, Refs. [35–49]). In this work we are interested in possible 4th generation effects on $B \rightarrow K^* \ell \ell$, specifically on the ratio $\mathcal{R}[4]$. The two parameters that control SM4 effects on the magnetic and semileptonic coefficients are the mass of the 4th generation top quark, $m_{t'}$, and the ratio of CKM₄ elements $\lambda_{tt'}^s \equiv V_{t'b} V_{t's} / V_{tb} V_{ts}^*$. From the analyses in Refs. [44, 45] we extract ranges for these two parameters that are phenomenologically viable; in the numerical analysis we take $m_{t'} = 500$ GeV and $|\lambda_{tt'}^s| < 0.1$.

The SM4 expressions for the t' contributions to the Wilson coefficients C_{7-10} can be obtained trivially from the corresponding SM expressions. Since we are interested in the forward-backward asymmetry in $B \rightarrow K^* \ell \ell$, we do not need separately the combinations $V_{t'b} V_{t's}$ and $V_{tb} V_{ts}^*$, but only their ratio.

In Fig. 5 we show the dependence of $\mathcal{R}[4]$ on the magnitude and phase of $\lambda_{tt'}^s$ for $m_{t'} = 500$ GeV. It is clear that large deviations are possible though only in presence of large phases

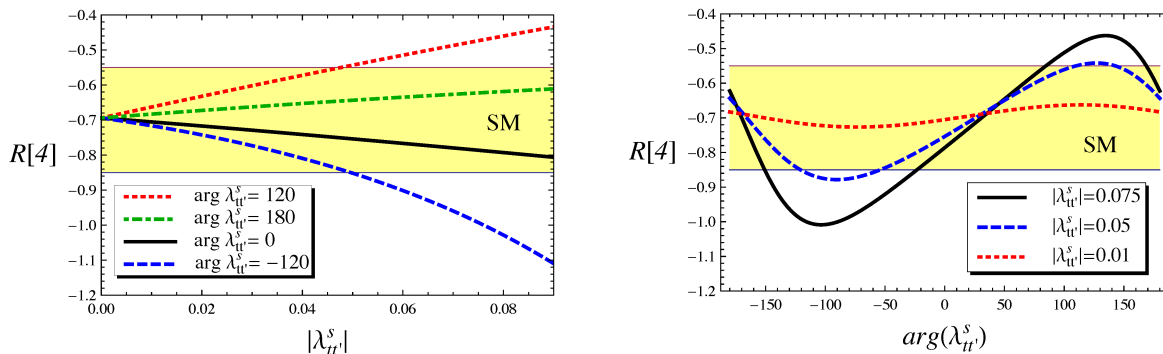


Figure 5: Expectations for $\mathcal{R}[4]$ in SM4. We fix the mass of the t' to 500 GeV and allow the ratio of CKM₄ elements $\lambda_{tt'}^s$ to vary according to the bounds obtained in Refs. [44, 45].

in the new CKM₄ elements.

This strong dependence on the CP violating phase of $\lambda_{tt'}^s$ stems entirely from the 4th generation contributions to C_{10} . In fact, the functional dependence of $\delta C_9^{4\text{th}}$ and $\delta C_{10}^{4\text{th}}$ on $m_{t'}$ is such that for large t' masses (in the range [200, 1000]GeV) one has $2 \lesssim |\delta C_{10}^{4\text{th}}/\delta C_9^{4\text{th}}| \lesssim 10$.

4.2 MSSM

Let us consider an R -parity conserving MSSM with non-vanishing sources of flavor changing neutral currents in the down squark sector (i.e. non Minimal Flavor Violating). As an example, we focus on contributions induced by a non-vanishing value of the LR mixing between the second and third generation. Adopting the formalism of Ref. [50] we define this mixing in the super-CKM basis (a basis in which the squark mass matrices are subject to the same rotations that diagonalize the regular quark sector).

In this model, gluino vertices are flavor changing and the dominant contributions to the Wilson coefficients come from 1-loop involving gluino and down squarks. The parameter that we need are the gluino and down squark masses and the mass insertion $(\delta_{23}^d)_{LR}$ (see Ref. [50] for more details).

The dominant constraints on this insertion come from $B \rightarrow X_s \gamma$, $B \rightarrow X_s \ell \ell$, B_s mixing, vacuum stability and absence of color breaking minima in the potential. The interplay of these constraints and the allowed ranges for $(\delta_{23}^d)_{LR}$ have been studied at length in the literature. In this work we use the results of Ref. [51]. Note that in Ref. [51] the bounds are given for $m_{\tilde{q}} \simeq m_{\tilde{g}} \simeq 350$ GeV and can be easily rescaled to cover the $m_{\tilde{q}} \simeq m_{\tilde{g}} \simeq 500$ GeV that we consider here.

In Fig. 6 we show the size of supersymmetric corrections to $\mathcal{R}[4]$. The opposite sign solution for the $B \rightarrow X_s \gamma$ amplitude (i.e. the $C_7 > 0$ scenario) requires a very large mass insertion, $(\delta_{23}^d)_{LR} \sim -0.08 \times (m_{\tilde{q}}/500 \text{ GeV})$, that is excluded by the charge and color breaking bound that reads $|(\delta_{23}^d)_{LR}| \lesssim 0.017 \times (m_{\tilde{q}}/500 \text{ GeV})$. On the other hand, the dependence of $\mathcal{R}[4]$ on the phase of the mass insertion is not as strong as in the 4th generation case. The reason for this is that in this supersymmetric model we do not have large contributions to C_{10} ; therefore,

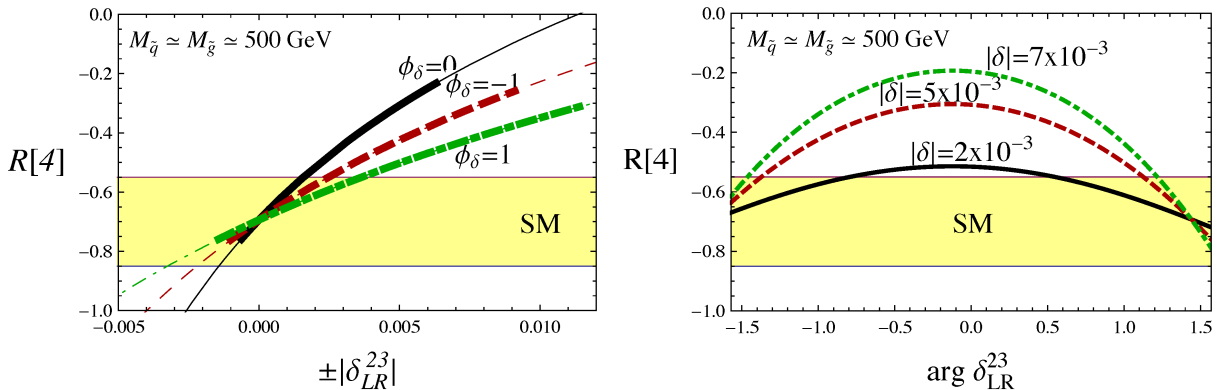


Figure 6: Dependence of $\mathcal{R}[4]$ on $|\delta_{23}^{LR}|$ for $m_{\tilde{g}} \simeq m_{\tilde{q}} \simeq 500$ GeV. We indicate with a thicker line the region allowed by $B \rightarrow X_s \gamma$. Solid, dashed and dot-dashed lines correspond to various values of ϕ_δ and $|\delta_{23}^{LR}|$.

the mechanism (see Eq. (27)) that induces a large sensitivity to CP violating phases in $\mathcal{R}[4]$ is not active in this case.

4.3 Family–dependent $U(1)'$

As a final example of new physics scenarios in which the observable $\mathcal{R}[4]$ has a strong discriminating power, we consider a Z' model with tree–level flavor changing couplings proposed and analyzed in Ref. [52] (see also Ref. [53] for an analysis of an effective flavor changing $Z\bar{b}s$ coupling). In this analysis we assume that the $U(1)'$ coupling constant (g_2 in the notation of Ref. [52]) is identical to the SM $U(1)$ coupling g_1 and that the Z and Z' have identical couplings to leptons. Therefore, the only parameters that remain (for what concerns $b \rightarrow s$ transitions) are the Z' mass and the flavor changing complex couplings $B_{bs}^{L,R}$, defined as

$$\mathcal{L}_{FC} = -g_2 Z'_\mu \bar{b} \gamma^\mu [B_{bs}^L P_L + B_{bs}^R P_R] s. \quad (31)$$

The effect of B_{bs}^R is to generate contributions to the operators $O'_{9,10}$ obtained from $O_{9,10}$ by replacing the left–handed quark current with a right–handed one. In our study we will not consider this possibility and assume that Z' couplings follow the weak interactions chiral structure (i.e. we take $B_{bs}^R = 0$). Utilizing Eq. (31) we obtain:

$$\delta C_9 = -\frac{4s_W^2 - 1}{2} \left(V_{tb} V_{ts}^* \frac{\alpha_{\text{em}}}{4\pi} \right)^{-1} \frac{g_2 m_Z}{g_1 m_{Z'}} \hat{B}_{bs}^L, \quad (32)$$

$$\delta C_{10} = -\frac{1}{2} \left(V_{tb} V_{ts}^* \frac{\alpha_{\text{em}}}{4\pi} \right)^{-1} \frac{g_2 m_Z}{g_1 m_{Z'}} \hat{B}_{bs}^L, \quad (33)$$

where s_W is the weak mixing angle and, following Ref. [52], we defined[§] $\hat{B}_{bs}^L \equiv B_{bs}^L (g_2 m_Z / g_1 m_{Z'})$. The reason for replacing B_{bs}^L with the $m_{Z'}$ dependent coupling \hat{B}_{bs}^L is that the latter is directly

[§]In Ref. [52] the rescaling of the B couplings is performed but the hat symbol is not explicitly introduced.

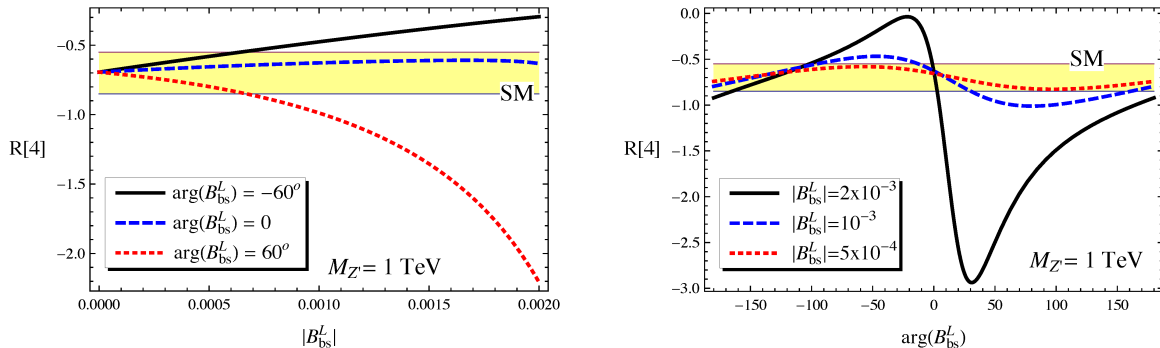


Figure 7: Expectations for $\mathcal{R}[4]$ in a family-dependent $U(1)'$ model. We fix the mass of the Z' to 1 TeV, allow the complex parameter $|B_{bs}^L| < 2 \times 10^{-3}$ [52] and assume that the Z' coupling to leptons is identical to the SM.

constrained by data on B_s mixing and $B \rightarrow (\pi, \psi, \phi, \eta', \rho, \omega, f^0)K_S$ decays: the authors of Ref. [52] find that these constraints result into the upper bound $|\hat{B}_{bs}^L| \lesssim 2 \times 10^{-3}$. From the inspection of Eqs. (32) and (33) it is clear that the exchange of a Z' generates only sizable contributions to C_{10} . In fact, as a direct consequence of our assumptions of identical Z and Z' couplings to leptons we have $\delta C_9 / \delta C_{10} = 4s_W^2 - 1 \simeq -0.075$. For this reason we expect large contributions to $\mathcal{R}[4]$ only for (large) non-zero values of the \hat{B}_{bs}^L phase.

We present the results of our numerical analysis in Fig. 7, where we show the dependence of $\mathcal{R}[4]$ on the modulus and phase of \hat{B}_{bs}^L for $m_{Z'} = 1$ TeV. Clearly very large effects are possible and a measurement of $\mathcal{R}[4]$, together with CP violation in B_s mixing and $b \rightarrow sq\bar{q}$ modes can provide a smoking gun for these models.

5 Conclusions

In this paper we introduce a new observable in exclusive $B \rightarrow K^* \ell^+ \ell^-$ and $B_s \rightarrow \phi \ell^+ \ell^-$ decays: the ratio $\mathcal{R}[4]$ of the integrated forward-backward asymmetry in the $[4, 6]\text{GeV}^2$ and $[1, 4]\text{GeV}^2$ bins. The separation between the two bins roughly coincides with the position of the zero of the FB asymmetry spectrum (calculated in the SM at NLO).

We have shown that the bulk of the theoretical uncertainty on $\mathcal{R}[4]$ is due to perturbative scale uncertainties and that the form factor dependence drops out almost completely. This ratio is therefore extremely interesting because its SM prediction Eq. (22) can be systematically improved without requiring any non-perturbative input. The position of the zero of the spectrum shares these positive features and can be determined with even better theoretical accuracy, but is much harder to measure.

A very interesting feature of $\mathcal{R}[4]$ is the strong dependence on the CP violating phases (especially those appearing in the Wilson coefficient C_{10}). This dependence arises because of the presence of strong phases in the $b \rightarrow s \ell^+ \ell^-$ matrix elements of current-current and QCD penguin operators (i.e. O_{1-6}). The latter can be determined perturbatively using QCD

factorization (or SCET).

We performed a model independent study of new physics contributions to the coefficients $C_{7,9,10}$ and specialized the analysis to several concrete new physics models. We find that, after imposing the constraints from experimental data on radiative and semileptonic rare decays, there are two scenarios in which large effects are possible.

- Models with modest (large) contributions to the coefficients C_7 (C_9). As a representative of this class we considered an MSSM with non-vanishing $(\delta_{23}^D)_{LR}$ mass insertion. In this case, large effects on $\mathcal{R}[4]$ and on the location of the zero are correlated. Moreover, we do not find a very strong dependence on the new physics phases of $\delta C_{7,9}$.
- Models with large and complex contributions to C_{10} . We considered the inclusion of a sequential 4th generation to the SM (SM4) and a $U(1)'$ model with family-dependent couplings (i.e. tree-level flavor changing Z' interactions). In SM4 we find large contributions to C_{10} because of the loop-function dependence on the t' mass; in the family dependent $U(1)'$ model this behavior is a result of our assumption of universal Z and Z' couplings to leptons. In these models we find very large effects on $\mathcal{R}[4]$ driven by the phase of δC_{10} . At the same time there is almost no change in the position of the zero of the spectrum because new physics contributions to C_{10} do not impact this observable at all.

In conclusion, we believe that this new observable should be promptly included in future experimental studies of $B \rightarrow K^* \ell \ell$ decays because it allows for an easier access (i.e. less luminosity is required) to the new physics probed by the zero of the spectrum and, at the same time, is sensitive to the quite elusive new physics phase in C_{10} .

Acknowledgments

This research was supported in part by the U.S. DOE contract No.DE-AC02-98CH10886(BNL).

References

- [1] W. S. Hou, R. S. Willey and A. Soni, Phys. Rev. Lett. **58**, 1608 (1987)
- [2] T. Hurth and M. Nakao, arXiv:1005.1224 [hep-ph].
- [3] T. E. Browder, T. Gershon, D. Pirjol, A. Soni and J. Zupan, Rev. Mod. Phys. **81**, 1887 (2009) [arXiv:0802.3201 [hep-ph]].
- [4] U. Egede, T. Hurth, J. Matias, M. Ramon and W. Reece, arXiv:1005.0571 [hep-ph].
- [5] E. Barberio *et al.* [Heavy Flavor Averaging Group], arXiv:0808.1297 [hep-ex] and online update at <http://www.slac.stanford.edu/xorg/hfag>.
- [6] M. Artuso, E. Barberio and S. Stone, PMC Phys. A **3**, 3 (2009) [arXiv:0902.3743 [hep-ph]].

- [7] T. Huber, T. Hurth and E. Lunghi, arXiv:0807.1940 [hep-ph].
- [8] T. Huber, E. Lunghi, M. Misiak and D. Wyler, Nucl. Phys. B **740**, 105 (2006).
- [9] T. Huber, T. Hurth and E. Lunghi, Nucl. Phys. B **802**, 40 (2008) [arXiv:0712.3009 [hep-ph]].
- [10] See, *e.g.* A. Ali, E. Lunghi, C. Greub and G. Hiller, Phys. Rev. D **66**, 034002 (2002) [arXiv:hep-ph/0112300].
- [11] B. Aubert *et al.* [BABAR Collaboration], Phys. Rev. D **79**, 031102 (2009) [arXiv:0804.4412 [hep-ex]].
- [12] J. T. Wei *et al.* [BELLE Collaboration], Phys. Rev. Lett. **103**, 171801 (2009) [arXiv:0904.0770 [hep-ex]].
- [13] CDF Collaboration, public note 10047.
- [14] W. Altmannshofer, P. Ball, A. Bharucha, A. J. Buras, D. M. Straub and M. Wick, JHEP **0901**, 019 (2009).
- [15] M. Beneke, T. Feldmann and D. Seidel, Nucl. Phys. B **612**, 25 (2001).
- [16] M. Beneke, T. Feldmann and D. Seidel, Eur. Phys. J. C **41**, 173 (2005).
- [17] P. Ball and R. Zwicky, JHEP **0604**, 046 (2006).
- [18] F. Kruger and J. Matias, Phys. Rev. D **71**, 094009 (2005).
- [19] E. Lunghi and J. Matias, JHEP **0704**, 058 (2007).
- [20] M. Beneke and T. Feldmann, Nucl. Phys. B **592**, 3 (2001).
- [21] C. W. Bauer, Z. Ligeti, M. Luke, A. V. Manohar and M. Trott, Phys. Rev. D **70**, 094017 (2004).
- [22] C. Amsler *et al.* (Particle Data Group), Phys. Lett. B **667** (2008) 1 and 2009 partial update for the 2010 edition.
- [23] J. Laiho, E. Lunghi and R. S. Van de Water, Phys. Rev. D **81**, 034503 (2010).
- [24] P. Ball and R. Zwicky, JHEP **0602**, 034 (2006);
P. Ball and G. W. Jones, JHEP **0703**, 069 (2007);
P. Ball, V. M. Braun and A. Lenz, JHEP **0708**, 090 (2007).
- [25] M. Bander, D. Silverman and A. Soni, Phys. Rev. Lett. **43**, 242 (1979).
- [26] F. Kruger and E. Lunghi, Phys. Rev. D **63**, 014013 (2001) [arXiv:hep-ph/0008210].

- [27] S. Chen *et al.* [CLEO Collaboration], Phys. Rev. Lett. **87**, 251807 (2001) [arXiv:hep-ex/0108032].
- [28] K. Abe *et al.* [Belle Collaboration], Phys. Lett. B **511**, 151 (2001) [arXiv:hep-ex/0103042].
- [29] B. Aubert *et al.* [BABAR Collaboration], Phys. Rev. D **72**, 052004 (2005) [arXiv:hep-ex/0508004].
- [30] B. Aubert *et al.* [BaBar Collaboration], Phys. Rev. Lett. **97**, 171803 (2006) [arXiv:hep-ex/0607071].
- [31] B. Aubert *et al.* [BABAR Collaboration], Phys. Rev. D **77**, 051103 (2008) [arXiv:0711.4889 [hep-ex]].
- [32] A. Limosani *et al.* (BELLE), presented at Moriond E.W. (2008).
- [33] B. Aubert *et al.* [BABAR Collaboration], Phys. Rev. Lett. **93**, 081802 (2004) [arXiv:hep-ex/0404006].
- [34] M. Iwasaki *et al.* [Belle Collaboration], Phys. Rev. D **72**, 092005 (2005) [arXiv:hep-ex/0503044].
- [35] G. D. Kribs, T. Plehn, M. Spannowsky and T. M. P. Tait, Phys. Rev. D **76**, 075016 (2007) [arXiv:0706.3718 [hep-ph]].
- [36] A. Soni, A. K. Alok, A. Giri, R. Mohanta and S. Nandi, Phys. Lett. B **683**, 302 (2010).
- [37] B. Holdom, W. S. Hou, T. Hurth, M. L. Mangano, S. Sultansoy and G. Unel, PMC Phys. A **3**, 4 (2009) [arXiv:0904.4698 [hep-ph]].
- [38] W. S. Hou and C. Y. Ma, arXiv:1004.2186 [hep-ph].
- [39] M. Bobrowski, A. Lenz, J. Riedl and J. Rohrwild, Phys. Rev. D **79**, 113006 (2009) [arXiv:0902.4883 [hep-ph]].
- [40] O. Eberhardt, A. Lenz and J. Rohrwild, arXiv:1005.3505 [hep-ph].
- [41] M. S. Chanowitz, Phys. Rev. D **79**, 113008 (2009) [arXiv:0904.3570 [hep-ph]].
- [42] G. Eilam, B. Melic and J. Trampetic, Phys. Rev. D **80**, 116003 (2009) [arXiv:0909.3227 [hep-ph]].
- [43] S. Bar-Shalom, G. Eilam and A. Soni, Phys. Lett. B **688**, 195 (2010) [arXiv:1001.0569 [hep-ph]].
- [44] A. Soni, A. K. Alok, A. Giri, R. Mohanta and S. Nandi, arXiv:1002.0595 [hep-ph].

- [45] A. J. Buras, B. Duling, T. Feldmann, T. Heidsieck, C. Promberger and S. Recksiegel, arXiv:1002.2126 [hep-ph].
- [46] A. J. Buras, B. Duling, T. Feldmann, T. Heidsieck, C. Promberger and S. Recksiegel, arXiv:1004.4565 [hep-ph].
- [47] A. J. Buras, B. Duling, T. Feldmann, T. Heidsieck and C. Promberger, arXiv:1006.5356 [hep-ph].
- [48] D. Choudhury and D. K. Ghosh, arXiv:1006.2171 [hep-ph].
- [49] M. S. Chanowitz, arXiv:1007.0043 [hep-ph].
- [50] E. Lunghi, A. Masiero, I. Scimemi and L. Silvestrini, Nucl. Phys. B **568**, 120 (2000).
- [51] L. Silvestrini, Ann. Rev. Nucl. Part. Sci. **57**, 405 (2007) [arXiv:0705.1624 [hep-ph]].
- [52] V. Barger, L. L. Everett, J. Jiang, P. Langacker, T. Liu and C. E. M. Wagner, JHEP **0912**, 048 (2009) [arXiv:0906.3745 [hep-ph]].
- [53] G. Hiller, Phys. Rev. D **66**, 071502 (2002) [arXiv:hep-ph/0207356].